

Calculating the reflectance map

Berthold K. P. Horn and Robert W. Sjöberg

It appears that the development of machine vision may benefit from a detailed understanding of the imaging process. The reflectance map, showing scene radiance as a function of surface gradient, has proved to be helpful in this endeavor. The reflectance map depends both on the nature of the surface layers of the objects being imaged and the distribution of light sources. Recently, a unified approach to the specification of surface reflectance in terms of both incident and reflected beam geometry has been proposed. The reflecting properties of a surface are specified in terms of the bidirectional reflectance-distribution function (BRDF). Here we derive the reflectance map in terms of the BRDF and the distribution of source radiance. A number of special cases of practical importance are developed in detail. The significance of this approach to the understanding of image formation is briefly indicated.

I. Reflectance Map

The apparent brightness of a surface patch depends on the orientation of the patch relative to the viewer and the light sources. Different surface elements of a nonplanar object will reflect different amounts of light toward an observer as a consequence of their differing attitude in space. A smooth opaque object will thus give rise to a shaded image, in which brightness varies spatially, even though the object may be illuminated evenly and covered by a uniform surface layer. This shading provides important information about the object's shape and has been exploited in machine vision.¹⁻⁸

A convenient representation for the relevant information is the "reflectance map".^{4,6} The reflectance map, $R(p,q)$, gives scene radiance as a function of surface gradient (p,q) in a viewer-centered coordinate system. If z is the elevation of the surface above a reference plane lying perpendicular to the optical axis of the imaging system, and if x and y are distances in this plane measured parallel to orthogonal coordinate axes in the image, p and q are the first partial derivatives of z with respect to x and y : $p = \partial z / \partial x$ and $q = \partial z / \partial y$.

The reflectance map is usually depicted as a series of contours of constant scene radiance (Fig. 1). It can be measured directly using a goniometer-mounted sample, or indirectly from the image of an object of known shape. Alternatively, a reflectance map may be cal-

culated if properties of the surface material and the distribution of light sources are given. One purpose of this paper is to provide a systematic approach to this latter endeavor. Another is to derive the relationship between scene radiance and image irradiance in an imaging system. This is relevant to machine vision since gray levels are quantized measurements of image irradiance.

II. Microstructure of Surfaces

When a ray of light strikes the surface of an object it may be absorbed, transmitted, or reflected. If the surface is flat and the underlying material homogeneous, the reflected ray will lie in the plane formed by the incident ray and the surface normal and will make an angle with the local normal equal to the angle between the incident ray and the local normal. This is referred to as specular, metallic, or dielectric reflection. Objects with surfaces of this kind form virtual images of surrounding objects.

Many surfaces are not perfectly flat on a microscopic scale and thus scatter parallel incident rays into a variety of directions (Fig. 2). If deviations of the local surface normals from the average are small, most of the rays will lie near the direction for ideal specular reflection and contribute to a surface shine or gloss.

Other surface layers are not homogeneous on a microscopic scale and thus scatter light rays which penetrate the surface by refraction and reflection at boundaries between regions with differing refractive indices (Fig. 3). Scattered rays may reemerge near the point of entry with a variety of directions and so contribute to diffuse, flat, or matte reflection. Snow and layers of white paint are examples of surfaces with this kind of behavior. Frequently both effects occur in

The authors are with MIT Artificial Intelligence Laboratory, Cambridge, Massachusetts 02139.

Received 27 January 1979.

0003-6935/79/111770-10\$00.50/0.

© 1979 Optical Society of America.

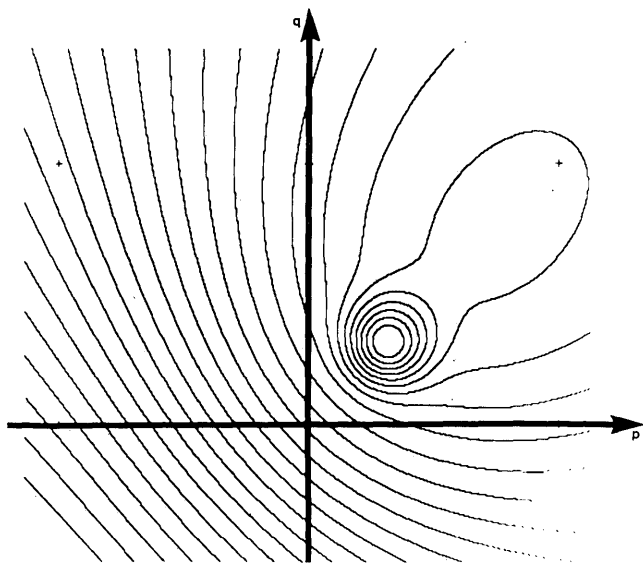


Fig. 1. A typical reflectance map for a surface, with both a glossy and a matte component of reflection, illuminated by a point source. The coordinates are surface slope in the x and y directions, and the curves shown are contours of constant scene radiance.

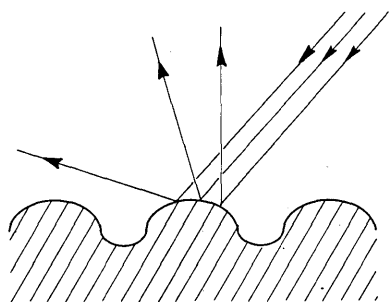


Fig. 2. Undulations in a specularly reflecting surface causing scattering of incident rays into a variety of directions. The surface will not appear specular if it is imaged on a scale where the surface undulations are not resolved. It may instead have a glossy appearance.

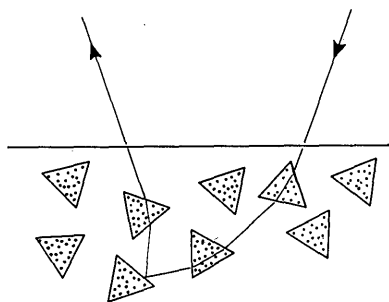


Fig. 3. Inhomogeneities in refractive index of surface layer components cause incident rays to be scattered into a variety of directions upon reflection. This kind of surface microstructure gives rise to matte reflection.

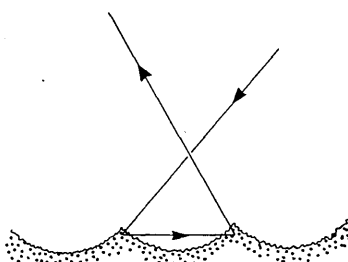


Fig. 4. Compound surface illustrating more complex model of interaction of light rays with surface microstructure.

surface layers, with some rays reflected at the nearly flat outer surface of the object, while others penetrate deeper and reemerge after multiple refractions and reflections in the inhomogeneous interior.

The distribution of reflected light in each case above depends on the direction of incident rays and the details of the microstructure of the surface layer. Naturally, what constitutes microstructure depends on one's point of view. Surface structures not resolved in a particular imaging situation are taken here to be microstructure. When viewing the moon through a telescope, for example, smaller hillocks and craterlets are part of this microstructure. This consideration leads to more complicated models of interaction of light with surfaces than those discussed so far. It is possible, for instance, to consider an undulating surface covered with a material, which in itself already has complicated reflecting behavior (Fig. 4).

Reflectance is not altered by rotating a surface patch about its normal when there is no asymmetry or preferred direction to either the pattern of surface undulations or the distribution of subsurface inhomogeneities. Many surface layers behave this way and permit a certain degree of simplification of the analysis. Exceptions are such things as diffraction gratings, iridescent plumage, and the mineral called tiger eye. These all have a distinct directionality in their surface microstructure and will not be considered here further.

Considerable attention has been paid to the reflective properties of various surface layers. Some researchers have concentrated on the experimental determination of surface reflectance properties.⁹⁻²¹ At the same time, many models have been developed for surface layers based on some of the considerations presented above.²²⁻³⁵ Models often are too simple to be realistic, or too complicated to yield solutions in closed form. In the latter case, Monte Carlo methods can be helpful, although they lead only to numerical specification of the reflecting behavior. Purely phenomenological models of reflectance have found favor in the computer graphics community.³⁶⁻³⁸ Several books have appeared describing the uses of reflectance measurements in determining basic optical properties of the materials in-

volved.³⁹⁻⁴¹ Attention has been paid, too, to the problem of making precise the definitions of reflectance and related concepts.^{42,43}

III. Radiometry

A modern precise nomenclature for radiometric terms has been promoted by a recent NBS publication.⁴³ Table I gives the terms, preferred symbols, and unit dimensions of the radiometric concepts we will have occasion to use for the development presented here.

Radiant flux Φ is the power propagated as optical electromagnetic radiation and is measured in watts (W). The radiant intensity I of a source is the exitant flux per unit solid angle and is measured in watts per steradian ($W \cdot sr^{-1}$). The total flux emitted by a source is the integral of radiant intensity over the full sphere of possible directions (4π sr). The irradiance E is the incident flux density, while radiant exitance M is the exitant flux density, both measured in watts per square meter of surface ($W \cdot m^{-2}$). The total radiant exitance equals the total irradiance if the surface reflects all incident light, absorbing and transmitting none.

The radiance L is the flux emitted per unit foreshortened surface area per unit solid angle. Radiance is measured in watts per square meter per steradian ($W \cdot m^{-2} \cdot sr^{-1}$). It can equivalently be defined as the flux emitted per unit surface area per unit projected solid angle. Radiance is an important concept since the apparent brightness of a surface patch is related to its radiance. Specifically, image irradiance will be shown to be proportional to scene radiance.

Radiance is a directional quantity. If the angle between the surface normal and the direction of exitant radiation is θ , the foreshortened area is the actual surface area times the cosine of this angle θ . Similarly the projected solid angle is the actual solid angle times the cosine of the angle θ . Here we will use the symbol ω to denote a solid angle, while Ω will be used to denote a projected solid angle. If $d\omega$ and $d\Omega$ are corresponding infinitesimal solid angles and projected solid angles, respectively, $d\Omega = d\omega \cdot \cos\theta$.

The following example (Fig. 5) will illustrate some of these ideas. Consider a source of radiation with intensity I in the direction of a surface patch of area dA , oriented with its surface normal making angle θ with the line connecting the patch to the source. In fact, as seen from the source, it appears only as a patch of area $dA \cdot \cos\theta$ would when oriented perpendicular to this line. The corresponding solid angle is simply the area of this equivalent patch divided by the square of the distance from the source to the patch. Thus,

$$d\omega = dA \cdot \cos\theta / r^2$$

The flux intercepted then is

$$d\Phi = I \cdot d\omega = I \cdot dA \cdot \cos\theta / r^2$$

The irradiance of the surface is just the incident flux divided by the area of the surface patch:

$$E = d\Phi / dA = I \cdot \cos\theta / r^2$$

Table I. Radiometric Concepts

Radiant flux	Φ	W
Radiant intensity	$I = d\Phi/d\omega$	$W \cdot sr^{-1}$
Irradiance	$E = d\Phi/dA$	$W \cdot m^{-2}$
Radiant exitance	$M = d\Phi/dA$	$W \cdot m^{-2}$
Radiance	$L = d^2\Phi / (dA \cdot \cos\theta \cdot d\omega)$	$W \cdot m^{-2} \cdot sr^{-1}$

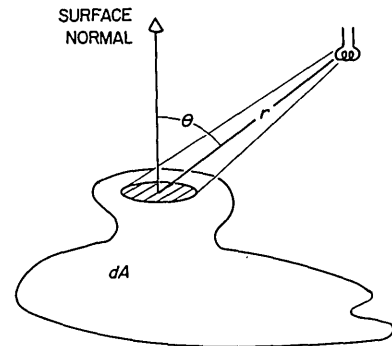


Fig. 5. Point source illuminating a surface, illustrating basic radiometric concepts.

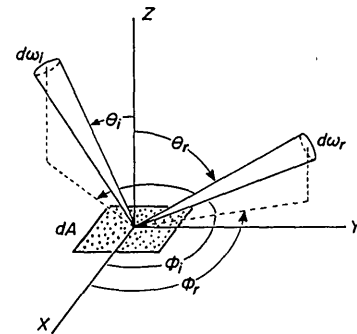


Fig. 6. Local geometry of incident and reflected rays needed for the definition of the bidirectional reflectance-distribution function (BRDF) (redrawn from Ref. 43).

IV. Bidirectional Reflectance-Distribution Function

The Bidirectional Reflectance-Distribution Function (BRDF) was recently introduced by Nicodemus *et al.*⁴³ as a unified notation for the specification of reflectance in terms of both incident- and reflected-beam geometry. The BRDF is denoted by the symbol f_r and captures the information about how bright a surface will appear, viewed from a given direction, when it is illuminated from another given direction. To be more precise, it is the ratio of reflected radiance dL_r in the direction toward the viewer to the irradiance dE_i in the direction toward a portion of the source. In symbols,

$$f_r(\theta_i, \phi_i; \theta_r, \phi_r) = dL_r(\theta_i, \phi_i; \theta_r, \phi_r, E_i) / dE_i(\theta_i, \phi_i)$$

Here, θ and ϕ together indicate a direction, the subscript i denoting quantities associated with incident radiant flux, while the subscript r indicates quantities associated with reflected radiant flux.⁴³

The geometry is as depicted in the figure (Fig. 6). A surface-specific coordinate system is erected with one

axis along the local normal to the surface and another defining an arbitrary reference direction in the local tangent plane. Directions are specified by polar angle θ (colatitude) measured from the local normal and azimuth angle ϕ (longitude) measured anticlockwise from the reference direction in the surface. In general, incident flux may arrive from many portions of extended sources, so incident radiance $L_i(\theta_i, \phi_i)$ is a function of direction. If we consider the component of flux $d\Phi_i$ arriving on the surface patch of area dA from an infinitesimal solid angle $d\omega_i$ in the direction (θ_i, ϕ_i) we obtain

$$d\Phi_i = L_i \cdot \cos\theta_i \cdot d\omega_i \cdot dA = L_i \cdot d\Omega_i \cdot dA = dE_i \cdot dA,$$

where $dE_i = L_i \cdot \cos\theta_i \cdot d\omega_i$ is the incident irradiance contributed by the portion of the source found in the solid angle $d\omega_i$ in the direction (θ_i, ϕ_i) . Similarly, the radiant flux emitted into an infinitesimal solid angle $d\omega_r$ in the direction (θ_r, ϕ_r) :

$$d^2\Phi_r = dL_r \cdot \cos\theta_r \cdot d\omega_r \cdot dA = dL_r \cdot d\Omega_r \cdot dA,$$

where $dL_r(\theta_r, \phi_r)$ is the radiance in the direction (θ_r, ϕ_r) due to the reflection of the flux incident from direction (θ_i, ϕ_i) . The notation dX , where X is one of the radiometric quantities introduced in Sec. III, will always denote a directional quantity, that is, one which depends on either the incident or exitant direction. The notation d^2X will mean a bidirectional quantity, which depends on both the incident and exitant directions. Thus, the incident flux $d\Phi_i$ depends only on the direction of incidence, but the exitant flux $d^2\Phi_r$ depends on both the direction of emittance and (implicitly) on the direction of incidence.

From these values of incident and exitant flux, the BRDF is defined as follows:

$$f_r(\theta_i, \phi_i; \theta_r, \phi_r) = (d^2\Phi_r/d\Omega_r)/d\Phi_i = dL_r/dE_i$$

and thus has dimension inverse steradian (sr^{-1}). The BRDF allows one to obtain reflectance for any defined incident and reflected ray geometry simply by integrating over the specified solid angles.⁴³

V. Integrals over Solid Angles and Projected Solid Angles

The admitting aperture of an imaging system may occupy a significant solid angle when seen from the point of view of the objects being imaged. We will furthermore have to deal with extended sources. In both cases it is necessary to integrate various quantities over solid angles or projected solid angles. This can be accomplished by double integration with respect to the polar and azimuth angles (Fig. 7). If X is the quantity to be integrated, we have

$$\int_{\omega} X d\omega = \int_{-\pi}^{\pi} \int_0^{\pi/2} X \sin\theta d\theta d\phi$$

$$\int_{\Omega} X d\Omega = \int_{-\pi}^{\pi} \int_0^{\pi/2} X \cos\theta \sin\theta d\theta d\phi.$$

If, for example, $X = 1$ and the region of integration is the hemisphere above the object's surface,

$$\int_{\omega} X d\omega = \int_{-\pi}^{\pi} \int_0^{\pi/2} \sin\theta d\theta d\phi = 2\pi,$$

while

$$\int_{\Omega} X d\Omega = \int_{-\pi}^{\pi} \int_0^{\pi/2} (\frac{1}{2}) \sin 2\theta d\theta d\phi = \pi.$$

The latter result will be used in the discussion of perfectly diffuse reflectance.

VI. Perfectly Diffuse Reflectance

A perfectly diffuse or Lambertian surface appears equally bright from all directions, regardless of how it is irradiated, and reflects all incident light.⁴³ Thus the reflected radiance is isotropic, that is, L_r is constant, with the same value for all directions (θ_r, ϕ_r) . Also, the integral of reflected radiance over the hemisphere above the surface must equal the irradiance E . This implies that the BRDF for this ideal surface $f_{r,id}$ is constant and that the radiant exitance M equals the irradiance E . If the reflected radiance is L_r , the radiant exitance can be found by integration:

$$M = \int_{\Omega_r} L_r d\Omega_r = L_r \pi.$$

From this one finds that

$$f_{r,id} = L_r/E_i = L_r/M = 1/\pi.$$

If we have an extended source with radiance L_i , the irradiance on the surface due to a small portion of solid angle $d\omega_i$ lying in the direction (θ_i, ϕ_i) is

$$dE_i(\theta_i, \phi_i) = L_i(\theta_i, \phi_i) \cos\theta_i d\omega_i.$$

The reflected radiance is then

$$L_r = (1/\pi) \int_{\omega} L_i(\theta_i, \phi_i) \cos\theta_i d\omega_i.$$

This is a form of Lambert's cosine law.

VII. Collimated Sources and the Dirac Delta Function

Not all sources are extended. One way to deal with sources that are highly collimated is to treat them as limiting cases of extended sources, with the distribution

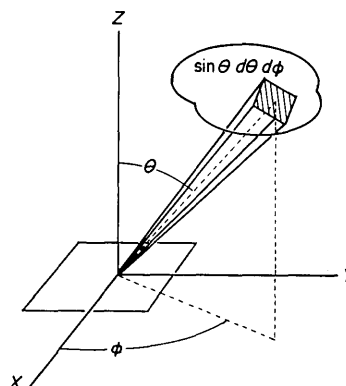


Fig. 7. Polar and azimuth angles used in double integrals over specified solid angles.

tending toward an impulse or delta function. If this is to be expressed in a coordinate system of polar and azimuth angles, one has to take into account the nonuniform spacing of coordinates. Consider a collimated source which produces an irradiance E_0 on a surface oriented orthogonally to the direction (θ_0, ϕ_0) of its rays. Clearly the radiance L_i of this source should be zero except for this direction. The product of Dirac delta functions, $\delta(\theta_i - \theta_0) \cdot \delta(\phi_i - \phi_0)$, will be a useful ingredient of the formula expressing L_i as a function of the angles. One must insure, however, that the irradiance on a surface lying orthogonal to the rays equals E_0 , that is,

$$E_0 = \int_{-\pi}^{\pi} \int_0^{\pi/2} L_i \sin\theta_i d\theta_i d\phi_i.$$

Clearly this can be accomplished if

$$L_i = E_0 \delta(\theta_i - \theta_0) \delta(\phi_i - \phi_0) / \sin\theta_0.$$

This is called the double-delta representation of source radiance for a collimated source. It can also be written in an alternate form using the identity

$$\delta[f(x) - f(x_0)] = \delta(x - x_0) / f'(x_0),$$

where $f'(x_0)$ is the derivative of $f(x)$ evaluated at $x = x_0$, provided that $f(x)$ has an inverse in the domain of interest. (This identity can be confirmed by integrating each side with respect to x over the relevant interval.) Then,

$$L_i = E_0 \delta(\cos\theta_i - \cos\theta_0) \delta(\phi_i - \phi_0).$$

VIII. Perfectly Specular Reflectance

A perfectly specular or mirrorlike surface reflects light rays in such a way that the exitant angle θ_r equals the incident angle θ_i and that the incident and reflected ray lie in a plane containing the surface normal. The reflected radiance of a surface patch in the direction (θ_r, ϕ_r) is simply the source radiance in the corresponding reflected direction. That is,

$$L_r(\theta_r, \phi_r) = L_i(\theta_r, \phi_r + \pi).$$

The surface thus forms a virtual image of the source. From the definition of the BRDF, we see that

$$L_r = \int f_r dE_i = \int_{\Omega_i} f_r L_i d\Omega_i.$$

That is,

$$L_r = \int_{-\pi}^{\pi} \int_0^{\pi/2} f_r L_i \cos\theta_i \sin\theta_i d\theta_i d\phi_i.$$

We can satisfy the conditions stated above if we let

$$f_{r, is} = \delta(\theta_i - \theta_r) \delta(\phi_i - \phi_r + \pi) / (\sin\theta_i \cos\theta_i).$$

This is called the double-delta form of the BRDF for perfectly specular reflectance. Using the identity mentioned in the last section, we can write this in an alternate form⁴³:

$$f_{r, is} = 2\delta(\sin^2\theta_r - \sin^2\theta_i) \delta(\phi_r - \phi_i + \pi).$$

IX. Analysis of Image-Forming System

We will now analyze a simple image-forming system (Fig. 8). We assume that the device is properly focused, that is, those rays originating from a particular point on the object which pass through the entrance aperture are deflected to meet at a single point in the image plane. Similarly, rays originating in the infinitesimal area dA_0 on the object's surface are projected into some area dA_p in the image plane, and no rays from other portions of the object's surface will reach this area of the image. Furthermore, we assume that there is no vignetting, that is, the entrance aperture is a constant circle of diameter d and does not become occluded for directions which make a larger angle with the optical axis. The effect of vignetting on image irradiance will be considered later.

The exposure of film in a camera is proportional to image irradiance E_p , and gray levels in a digital imaging system are quantized measurements of image irradiance. In order to calculate image irradiance we must first determine the flux $d\Phi_L$ passing through the entrance aperture arriving from the patch of area dA_0 on the object.

$$d\Phi_L = dA_0 \int_{\Omega_r} L_r d\Omega_r,$$

where Ω_r is the projected solid angle subtended by the aperture. We will also need to know the area dA_p of the image of the patch, since image irradiance E_p is the flux per unit area:

$$E_p = d\Phi_L / dA_p.$$

If θ'_r is the angle between the normal on the surface and the line to the entrance aperture nodal point, while α is the angle between this line and the optical axis, then, by equating solid angles,

$$(dA_0 \cos\theta'_r) / f_0^2 = (dA_p \cos\alpha) / f_p^2.$$

Consequently,

$$E_p = (f_0 / f_p)^2 \cos\alpha \int_{\omega_r} L_r (\cos\theta_r / \cos\theta'_r) d\omega_r.$$

Here the integral is over the solid angle occupied by the entrance aperture as seen from the patch on the surface.

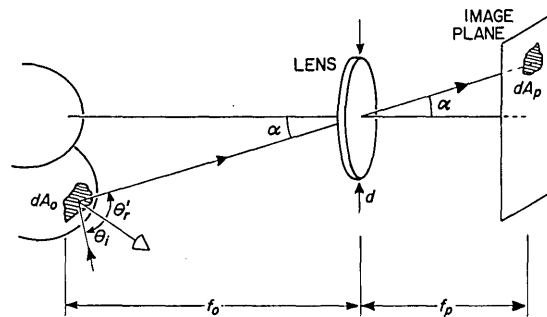


Fig. 8. A simple image-forming system. Light collected by the lens from the surface patch of area dA_0 is projected into the image patch of area dA_p .

If we assume that the lens is small relative to its distance from the object, θ_r is approximately the same as θ'_r , and the ratio of their cosines is unity. Furthermore, the reflected radiance L_r will then tend to be constant and can be removed from inside the integral. The solid angle occupied by the lens as seen from the surface patch is approximately equal to the foreshortened area $(\pi/4)d^2 \cos\alpha$, divided by the distance $(f_0/\cos\alpha)$ squared. Finally, one obtains the well-known result

$$E_p = L_r(\pi/4)(d/f_p)^2 \cos^4\alpha.$$

That is, image irradiance is proportional to scene radiance. The factor of proportionality is π divided by four times the effective f -number (f_p/d) squared times the fourth power of the cosine of the off-axis angle α . Thus the sensitivity of such an imaging system is not uniform over an image, but is constant for a particular point in the image. Vignetting introduces an additional variation with image position. Ideally, an imaging device should be calibrated so that this variation in sensitivity as a function of α can be removed.

Other kinds of imaging systems, such as microscopes or mechanical scanners, lead to somewhat different expressions. Generally, however, image irradiance is proportional to scene radiance in such systems too. At this point we should remember that scene radiance depends on properties of the surface layer (BRDF) and the distribution of light sources (source radiance) since

$$L_r = \int_{\Omega_i} f_r L_i d\Omega_i.$$

X. Viewer-Oriented Coordinate System

So far we have considered directions from the object to the image-forming system and to light sources in terms of a local coordinate system with one axis lined up with the surface normal. Such coordinate systems will vary in orientation from place to place and are thus inconvenient for the specification of global distributions such as that of source radiance. A coordinate system fixed in space will be more suitable, particularly if one of the axes is lined up with the optical axis (Fig. 9). In this viewer-oriented coordinate system we introduce polar angle θ measured from the z axis and azimuth angle ϕ measured from the x axis in the plane perpendicular to the z axis. Here, the z axis is parallel to the optical axis. Directions to sources of light can be given using these two angles. If the sources are far away in comparison to the size of the objects being imaged, source radiance will be a fixed function of these angles independent of the point on the surface being considered.

XI. Surface Normal

In the local coordinate system the surface normal lies along one of the axes, or equivalently, it is the direction corresponding to zero polar angle. In the viewer-oriented coordinate system the surface normal will correspond to some direction, say (θ_n, ϕ_n) . The corresponding unit vector is

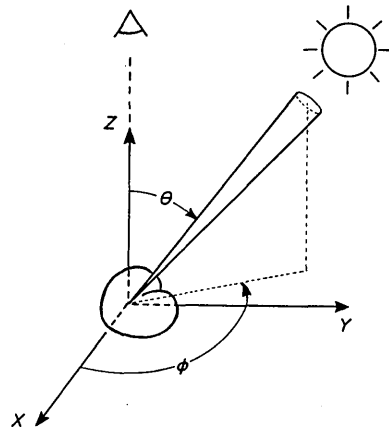


Fig. 9. Viewer-oriented global coordinate system useful for specification of the distribution of source radiance L_i .

$$\mathbf{n} = (\cos\phi_n \sin\theta_n, \sin\phi_n \sin\theta_n, \cos\theta_n).$$

The surface of the object may be specified by giving elevation z as a function of the coordinates x and y . We can give an expression for the surface normal in terms of the first partial derivatives of z with respect to x and y , if these exist. Let the first partial derivatives be called p and q . Then the vectors $(1,0,p)$ and $(0,1,q)$ are tangent to the surface, as can be seen by considering infinitesimal steps in the x and y direction. The surface normal is perpendicular to all vectors in the tangent plane and so is parallel to the cross-product of these two:

$$(1,0,p) \times (0,1,q) = (-p,-q,1).$$

Thus the unit normal can be written

$$\mathbf{n} = (-p,-q,1)/(1+p^2+q^2)^{1/2}.$$

The following results are obtained by equating terms in the two expressions for the surface normal:

$$\sin\theta_n = (p^2+q^2)^{1/2}/(1+p^2+q^2)^{1/2};$$

$$\cos\theta_n = 1/(1+p^2+q^2)^{1/2};$$

$$\sin\phi_n = -q/(p^2+q^2)^{1/2};$$

$$\cos\phi_n = -p/(p^2+q^2)^{1/2}.$$

Conversely,

$$p = -\cos\phi_n \tan\theta_n;$$

$$q = -\sin\phi_n \tan\theta_n.$$

XII. Relationship Between Local and Viewer-Oriented Coordinate Systems

In order to calculate the scene radiance, we will integrate the product of the BRDF and the source radiance over all incident directions. Since the BRDF is

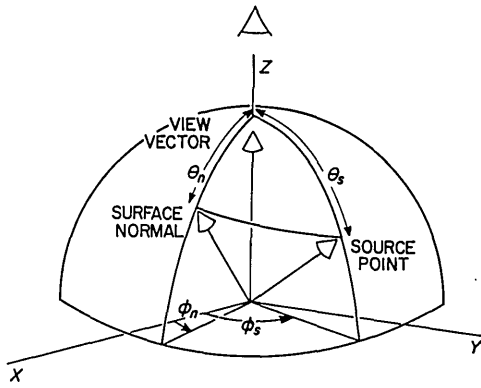


Fig. 10. Surface normal and direction to portion of the source shown in viewer-oriented coordinate system.

specified in terms of the local coordinate system, while the distribution of source radiance is likely to be given in the viewer-oriented coordinate system, it will be necessary to convert between the two. Given the direction of the surface normal (θ_n, ϕ_n) and the direction to a portion of the source (θ_s, ϕ_s) , both specified in the viewer-oriented system (Fig. 10), we have to find the incident direction (θ_i, ϕ_i) and the exitant direction (θ_r, ϕ_r) both specified in the local system. Alternatively, given the surface normal and the incident direction we may have to find the direction to the source and the exitant direction. Note that $\theta_r = \theta_n$ since the exitant ray lies along the z axis in the direction toward the viewer. Further, since we have excluded anisotropic surfaces, we are only interested in the difference between ϕ_r and ϕ_i . From the relevant spherical triangle (Fig. 11) we obtain:

Cosine formula:

$$\cos\theta_i = \cos\theta_s \cos\theta_n + \sin\theta_s \sin\theta_n \cos(\phi_s - \phi_n);$$

Sine formula:

$$\sin\theta_i \sin(\phi_r - \phi_i) = \sin\theta_s \sin(\phi_s - \phi_n);$$

Analog formula:

$$\sin\theta_i \cos(\phi_r - \phi_i) = \cos\theta_s \sin\theta_n - \sin\theta_s \cos\theta_n \cos(\phi_s - \phi_n).$$

The Jacobian of the transformation from (θ_s, ϕ_s) to (θ_i, ϕ_i) equals

$$(\partial\theta_i/\partial\theta_s)(\partial\phi_i/\partial\phi_s) - (\partial\theta_i/\partial\phi_s)(\partial\phi_i/\partial\theta_s) = (\sin\theta_s/\sin\theta_i).$$

(The Jacobian will be required below when converting a double integral with respect to one set of coordinates to one in terms of the other.) The above formulas allow us to find the incident direction from the source direction. Quite symmetrically, we can also obtain the source direction from the incident direction:

Cosine formula:

$$\cos\theta_s = \cos\theta_i \cos\theta_r + \sin\theta_i \sin\theta_r \cos(\phi_r - \phi_i);$$

Sine formula:

$$\sin\theta_s \sin(\phi_s - \phi_n) = \sin\theta_i \sin(\phi_r - \phi_i);$$

Analog formula:

$$\sin\theta_s \cos(\phi_s - \phi_n) = \cos\theta_i \sin\theta_r - \sin\theta_i \cos\theta_r \cos(\phi_r - \phi_i).$$

The Jacobian of the transformation from (θ_i, ϕ_i) to (θ_s, ϕ_s) equals

$$(\partial\theta_s/\partial\theta_i)(\partial\phi_s/\partial\phi_i) - (\partial\theta_s/\partial\phi_i)(\partial\phi_s/\partial\theta_i) = (\sin\theta_i/\sin\theta_s).$$

XIII. Scene Radiance

It follows from the definition of the BRDF that reflected radiance can be written as the integral

$$L_r = \int_{\Omega_i} f_r L_i d\Omega_i = \int_{\omega_i} f_r L_i \cos\theta_i d\omega_i$$

Using polar and azimuthal angles this becomes

$$L_r(\theta_n, \phi_n) = \int_{-\pi}^{\pi} \int_0^{\pi/2} f_r(\theta_i, \phi_i; \theta_r, \phi_r) L_i(\theta_s, \phi_s) \cos\theta_i \sin\theta_i d\theta_i d\phi_i.$$

Here we integrate over all possible incident directions (θ_i, ϕ_i) and calculate source direction (θ_s, ϕ_s) from the given surface normal (θ_n, ϕ_n) and the incident direction. The inner integral has the limits 0 to $\pi/2$ for θ_i , corresponding to directions within the hemisphere visible from the surface. The integration can be extended to the full sphere of directions if the integrand is forced to be zero when θ_i lies between $\pi/2$ and π . This can be accomplished by replacing $\cos\theta_i$ by $\max[0, \cos\theta_i]$. Hence

$$L_r = \int_{-\pi}^{\pi} \int_0^{\pi} f_r L_i \max[0, \cos\theta_i] \sin\theta_i d\theta_i d\phi_i.$$

Since the integral now is over the full sphere of directions, it can be easily rewritten using any other set of polar and azimuth angles. Using the viewer-oriented coordinate system, for example, we obtain

$$L_r = \int_{-\pi}^{\pi} \int_0^{\pi} f_r L_i \max[0, \cos\theta_i] \sin\theta_s d\theta_s d\phi_s,$$

that is,

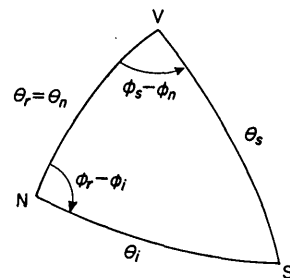


Fig. 11. Spherical triangle extracted from previous figure and used in derivation of transformation equations between the surface normal, local coordinate system, and the viewer-oriented, global coordinate system.

$$L_r(\theta_n, \phi_n) = \int_{-\pi}^{\pi} \int_0^{\pi} f_r(\theta_i, \phi_i; \theta_r, \phi_r) L_i(\theta_s, \phi_s) \times \max[0, \cos\theta_i] \sin\theta_s d\theta_s d\phi_s.$$

Here we integrate over all possible source directions (θ_s, ϕ_s) and calculate incident directions (θ_i, ϕ_i) from the given surface normal (θ_n, ϕ_n) and the source direction. We now have two convenient forms for the calculation of scene radiance. We proceed to calculate reflectance maps for a few simple combinations of BRDF and distributions of source radiance.

XIV. Lambertian Reflectance

A. Collimated Source

For a Lambertian reflector, $f_r = 1/\pi$. For a collimated source,

$$L_i = E_0 \delta(\theta_s - \theta_0) \delta(\phi_s - \phi_0) / \sin\theta_0,$$

where E_0 is the irradiance measured perpendicular to the beam of light arriving from source direction (θ_0, ϕ_0) . Substituting into the second form of the expression for scene radiance above, we obtain

$$L_r = \int_{-\pi}^{\pi} \int_0^{\pi} (E_0/\pi) \delta(\theta_s - \theta_0) \delta(\phi_s - \phi_0) \times \max[0, \cos\theta_i] (\sin\theta_s / \sin\theta_0) d\theta_s d\phi_s.$$

This is equal to

$$L_r = (E_0/\pi) \max[0, \cos\theta'_i],$$

where $\theta'_i = \theta_i$ when $\theta_s = \theta_0$ and $\phi_s = \phi_0$. In this case,

$$\cos\theta'_i = \cos\theta_r \cos\theta_0 + \sin\theta_r \sin\theta_0 \cos(\phi_0 - \phi_n)$$

and

$$\cos(\phi_0 - \phi_n) = \cos\phi_0 \cos\phi_n - \sin\phi_0 \sin\phi_n.$$

To obtain the reflectance map, scene radiance as a

function of surface gradient, we can substitute expressions in p and q for these trigonometric expressions. The result is

$$R(p, q) = (E_0/\pi) \max \left[0, \frac{(1 + p_0 p + q_0 q)}{(1 + p^2 + q^2)^{1/2} (1 + p_0^2 + q_0^2)^{1/2}} \right],$$

where

$$p_0 = -\cos\phi_0 \tan\theta_0,$$

$$q_0 = -\sin\phi_0 \tan\theta_0.$$

A surface with gradient (p_0, q_0) is normal to the direction of the incident light rays.

B. Uniform Source

A uniform source has constant incident radiance. Let $L_i = L_0$. Again, for a Lambertian reflector, $f_r = 1/\pi$. Substituting into the first form of the expression for scene radiance, we obtain

$$L_r = \int_{-\pi}^{\pi} \int_0^{\pi/2} (L_0/\pi) \cos\theta_i \sin\theta_i d\theta_i d\phi_i.$$

This becomes

$$L_r = L_0 \int_0^{\pi/2} \sin 2\theta_i d\theta_i = L_0.$$

Not surprisingly, the reflected radiance is independent of the surface orientation in this case.

C. Hemispherical Uniform Source

A hemispherical uniform source is described by

$$L_i(\theta_s, \phi_s) = L_0 \quad \text{for } \theta_s < \pi/2,$$

$$L_i(\theta_s, \phi_s) = 0 \quad \text{for } \theta_s > \pi/2.$$

In order to evaluate the double integral for scene radiance, it is necessary to know the value θ'_i of the incident angle θ_i , which corresponds to the horizon of the sky, that is, $\theta_s = \pi/2$. From the coordinate transformation equations one can easily see that

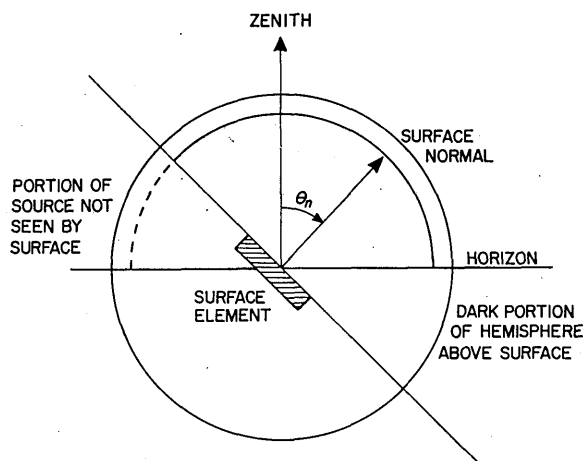


Fig. 12. Cross section through uniform hemispherical source and surface element, illustrating the horizon cutoff and the portion of extended source not visible from the surface.

$$\cot\theta'_i = -\tan\theta_r \cos(\phi_r - \phi_i).$$

For $\phi_r - \pi/2 < \phi_i < \phi_r + \pi/2$, the horizon cutoff only occurs for $\theta'_i > \pi/2$ and can be ignored, since the inner integral is from $\theta_i = 0$ to $\theta_i = \pi/2$ only. For the other half of the range of ϕ_i , this cutoff must be considered. Now,

$$L_r = \int_{-\pi}^{\pi} \int_0^{\pi/2} f_r L_i \cos\theta_i \sin\theta_i d\theta_i d\phi_i,$$

so

$$L_r = (L_0/\pi) \int_{-\pi}^{\pi} \int_0^{\min[\theta'_i, \pi/2]} \cos\theta_i \sin\theta_i d\theta_i d\phi_i.$$

Letting $\phi = \phi_i - \phi_r$ and $\phi' = \phi_i - \phi_r + \pi$, we can split the outer integral,

$$L_r = (L_0/\pi) \int_{-\pi/2}^{\pi/2} \int_0^{\pi/2} \cos\theta_i \sin\theta_i d\theta_i d\phi + (L_0/\pi) \int_{-\pi/2}^{\pi/2} \int_0^{\theta'_i} \cos\theta_i \sin\theta_i d\theta_i d\phi'.$$

Now

$$\int_0^{\pi/2} \cos\theta_i \sin\theta_i d\theta_i = 1/2,$$

so the first term is simply $L_0/2$. Next, note that

$$\int_0^{\theta'_i} \cos\theta_i \sin\theta_i d\theta_i = (1 - \cos 2\theta'_i)/4 = \sin^2\theta'_i/2,$$

where, since $\cot\theta'_i = -\tan\theta_r \cos(\phi_r - \phi_i)$,

$$\sin^2\theta'_i = 1/[1 + \tan^2\theta_r \cos^2(\phi_r - \phi_i)].$$

The second term thus becomes

$$(L_0/2\pi) \int_{-\pi/2}^{\pi/2} 1/(1 + \tan^2\theta_r \cos^2\phi') d\phi',$$

which equals

$$(L_0/2\pi) [\cos\theta_r \tan^{-1}(\cos\theta_r \tan\phi)]_{-\pi/2}^{\pi/2} = (L_0/2) \cos\theta_r.$$

Adding the two terms we finally get

$$L_r(\theta_n, \phi_n) = (L_0/2) (1 + \cos\theta_n) = L_0 \cos^2(\theta_n/2).$$

This is the result found by Brooks.⁴⁴ From it the reflectance map can be found immediately:

$$R(p, q) = (E_0/2)[1 + 1/(1 + p^2 + q^2)^{1/2}].$$

XV. Specular Reflectance

A. Collimated Source

For specular surfaces,

$$f_r = \delta(\theta_i - \theta_r)\delta(\phi_i - \phi_r + \pi)/(\sin\theta_i \cos\theta_i).$$

Using the source radiance from Sec. XIV. A and the first form of the expression for scene radiance, we obtain

$$L_r = \int_{-\pi}^{\pi} \int_0^{\pi/2} (L_0/\sin\theta_0)\delta(\theta_i - \theta_r)\delta(\phi_i - \phi_r + \pi) \times \delta(\theta_s - \theta_0)\delta(\phi_s - \phi_0)d\theta_i d\phi_i,$$

that is,

$$L_r = L_0\delta(\theta'_s - \theta_0)\delta(\phi'_s - \phi_0)/\sin\theta_0,$$

where θ'_s and ϕ'_s are the values of θ_s and ϕ_s corresponding to $\theta_i = \theta_r$ and $\phi_i = \phi_r + \pi$. Using the equations for the coordinate transformations, one finds that $\theta'_s = 2\theta_r$ and $\phi'_s = \phi_n$. Thus,

$$L_r = L_0\delta(2\theta_r - \theta_0)\delta(\phi_n - \phi_0)/\sin\theta_0$$

and finally

$$L_r(\theta_n, \phi_n) = (L_0/2)\delta(\theta_n - \theta_0/2)\delta(\phi_n - \phi_0)/\sin\theta_0.$$

To express this as a function of p and q we have to remember that

$$\delta[f(x, y) - f(x_0, y_0)]\delta[g(x, y) - g(x_0, y_0)] = \delta(x - x_0)\delta(y - y_0)/J(x_0, y_0),$$

where $J(x, y)$ is the Jacobian of the transformation from (x, y) to (f, g) (provided this transformation has an inverse in the region of interest):

$$J(x, y) = (\partial f/\partial x)(\partial g/\partial y) - (\partial f/\partial y)(\partial g/\partial x).$$

The Jacobian of the transformation from (p, q) to (θ_n, ϕ_n) is

$$J(p, q) = 1/[(p^2 + q^2)^{1/2} (1 + p^2 + q^2)].$$

Let

$$p_1 = -\cos\phi_0 \tan\theta_0/2,$$

$$q_1 = -\sin\phi_0 \tan\theta_0/2.$$

Then, noting that $\sin\theta_0 = 2 \sin(\theta_0/2) \cos(\theta_0/2)$, one can write

$$\sin\theta_0 = 2(p_1^2 + q_1^2)^{1/2}/(1 + p_1^2 + q_1^2),$$

and therefore

$$R(p, q) = (E_0/4)\delta(p - p_1)\delta(q - q_1)(1 + p_1^2 + q_1^2)^2.$$

Thus, a surface element with gradient (p_1, q_1) is oriented to reflect specularly the collimated source toward the viewer. This gradient can be related to the gradient (p_0, q_0) introduced earlier:

$$p_1 = p_0[(1 + p_0^2 + q_0^2)^{1/2} - 1]/(p_0^2 + q_0^2),$$

$$q_1 = q_0[(1 + p_0^2 + q_0^2)^{1/2} - 1]/(p_0^2 + q_0^2).$$

When the point (p_0, q_0) is not far from the origin, (p_1, q_1) is approximately midway between the origin and (p_0, q_0) .

B. Uniform Source

It is easy to see that for a specular surface under a uniform source, the scene radiance will be constant and equal to the source radiance: $L_r = L_0$. This is the same result as the one we obtained for the uniform source and Lambertian reflectance. Thus a diffuse surface appears just as bright as a specular surface if both are viewed with uniform illumination. In fact, all surfaces reflecting the same fraction, ρ say, of the total incident light will appear equally bright under this illumination condition.

C. Hemispherical Uniform Source

In this case,

$$L_r(\theta_n, \phi_n) = L_0 \quad \text{for } \theta_n < \pi/4,$$

$$L_r(\theta_n, \phi_n) = 0 \quad \text{for } \theta_n > \pi/4.$$

The reflectance map is

$$R(p, q) = L_0 \quad \text{for } p^2 + q^2 < 1,$$

$$R(p, q) = 0 \quad \text{for } p^2 + q^2 > 1.$$

XVI. Summary and Conclusions

We have shown that image irradiance is proportional to scene radiance and that scene radiance depends on surface orientation. The reflectance map gives scene radiance as a function of the gradient. It can be calculated from the bidirectional reflectance-distribution function (BRDF) and the distribution of source radiance. Several special cases were worked out in detail. Each could have been developed more easily by a direct method, but was obtained from the general expression for scene radiance to illustrate the technique. The general expression allows one to find the reflectance map even if the source radiance distribution or the BRDF is only given numerically.

The authors thank H.-H. Nagel, B. Neumann, B. Radig, and L. Dreschler of the University of Hamburg, who helped debug some of the ideas. Discussions with M. Brady and M. Brooks of the University of Essex were very helpful. Thanks go to P. Winston and K. Ikeuchi for helping proofread the manuscript. We are also grateful for text preparation by Blenda Horn and drawings by Karen Prendergast. Puma helped too.

This report describes research done at the Artificial Intelligence Laboratory of the Massachusetts Institute of Technology. Support for the Laboratory's artificial intelligence research is provided in part by the Advanced Research Projects Agency of the Department of Defense under Office of Naval Research contract N00014-75-C-0643.

References

1. J. van Diggelen, *Bull. Astron. Inst. Neth.* 11, No. 423 (1951).
2. T. Rindfleisch, *Photogramm. Eng.* 32, 262 (1966).
3. B. K. P. Horn, "Determining Shape from Shading," in *The Psychology of Computer Vision*, P. H. Winston, Ed. (McGraw-Hill, New York, 1975), Chap. 4.
4. B. K. P. Horn, *Artific. Intell.* 8, No. 11, 201 (1977).
5. R. J. Woodham, "A Cooperative Algorithm for Determining Surface Orientation from a Single View," in *Proceedings Fifth International Joint Conference on Artificial Intelligence*, MIT, Cambridge, Mass., August 1977, pp. 635-641.
6. R. J. Woodham, "Reflectance Map Techniques for Analyzing Surface Defects in Metal Castings," TR-457, Artificial Intelligence Laboratory, MIT, Cambridge, Mass. (1978).
7. R. J. Woodham, "Photometric Stereo: A Reflectance Map Technique for Determining Surface Orientation from Image Intensity," in *Proceedings of SPIE's 22nd Annual Technical Symposium* (SPIE, New York, 1978), Vol. 155, pp. 136-143.
8. B. K. P. Horn, R. J. Woodham, and W. N. Silver, "Determining Shape and Reflectance Using Multiple Images," A. I. Laboratory Memo 490, MIT, Cambridge, Mass. (August 1978).
9. F. H. Gilpin, *Trans. Illum. Eng. Soc.* 5, 854 (1910).
10. W. E. Knowles Middleton and A. G. Mungall, *J. Opt. Soc. Am.* 42, 572 (1952).
11. V. A. Fedoretz, *Publ. Kharkov Obs.* 2, 49 (1952).
12. J. van Diggelen, *Rech. Obs. Utrecht* 14, 1 (1959).
13. M. Minnaert, "Photometry of the Moon," in *Planets and Satellites, Vol. 3*, G. Kuiper and B. Middlehurst, Eds. (U. Chicago Press, Chicago, 1961), pp. 213-248.
14. V. Fesenkov, "Photometry of the Moon," in *Physics and Astronomy of the Moon*, Z. Kopal, Ed. (Academic, New York, 1962), pp. 99-130.
15. B. Hapke and H. Van Horn, *J. Geophys. Res.* 68, 4545 (1963).
16. G. de Vaucouleurs, *Icarus* 3, 187 (1964).
17. J. van Diggelen, *Planet. Space Sci.* 13, 271 (1965).
18. P. Oetking, *J. Geophys. Res.* 71, 2505 (1966).
19. J. J. Rennilson, H. E. Holt, and E. C. Morris, *J. Opt. Soc. Am.* 58, 747 (1968).
20. E. M. Patterson, C. E. Sheldon, and B. H. Stockton, *Appl. Opt.* 16, 729 (1977).
21. C. J. Tucker, *Appl. Opt.* 16, 1151 (1977).
22. M. Minnaert, *Astrophys. J.* 93, 403 (1941).
23. H. C. Van de Hulst, *Light Scattering by Small Particles* (Wiley, New York, 1957).
24. B. W. Hapke, *J. Geophys. Res.* 68, 4571 (1963).
25. N. T. Melamed, *J. Appl. Phys.* 34, 560 (1963).
26. B. Hapke, *Astron. J.* 71, 333 (1966).
27. K. E. Torrance, E. M. Sparrow, and R. C. Birkebak, *J. Opt. Soc. Am.* 56, 916 (1966).
28. K. E. Torrance and E. M. Sparrow, *J. Opt. Soc. Am.* 57, 1105 (1967).
29. T. S. Trowbridge and K. P. Reitz, *J. Opt. Soc. Am.* 65, 531 (1975).
30. E. L. Simmons, *Appl. Opt.* 14, 1380 (1975).
31. E. L. Simmons, *Opt. Acta* 22, 71 (1975).
32. E. L. Simmons, *J. Appl. Phys.* 46, 344 (1975).
33. E. L. Simmons, *Appl. Opt.* 15, 603 (1976).
34. C. J. Tucker and M. W. Garratt, *Appl. Opt.* 16, 635 (1977).
35. G. N. Plass, G. W. Kattawar, and J. A. Guinn, Jr., *Appl. Opt.* 16, 643 (1977).
36. H. Gouraud, "Computer Display of Curved Surfaces," Technical Report 113, UTEC-CSC-71, Computer Science, U. Utah, Salt Lake City (1971).
37. Bui Tuong-Phong, "Illumination for Computer-Generated Images," Technical Report 129, UTEC-CSC-73, Computer Science, U. Utah, Salt Lake City (1973).
38. J. F. Blinn, "Models of Light Reflection for Computer Synthesized Pictures," in *SIGGRAPH 77, Proceedings ACM, Computer Graphics* (July 1977), Vol. 11, No. 2, pp. 192-198.
39. W. W. Wendlandt and H. G. Hecht, *Reflectance Spectroscopy* (Interscience, New York, 1966).
40. W. W. Wendlandt, Ed., *Modern Aspects of Reflectance Spectroscopy* (Plenum, New York, 1968).
41. G. Kortuem, *Reflectance Spectroscopy*, J. E. Lohr, translator (Springer, Berlin, 1969).
42. D. E. Spencer and E. G. Gaston, *J. Opt. Soc. Am.* 65, 1129 (1975).
43. F. E. Nicodemus, J. C. Richmond, J. J. Hsia, I. W. Ginsberg, T. Limperis, "Geometrical Considerations and Nomenclature for Reflectance," NBS Monograph 160 (National Bureau of Standards, Washington, D.C., October 1977).
44. M. J. Brooks, "Investigating the Effects of Planar Light Sources," CSM 22, Department of Computer Science, Essex University, Colchester, England (1978).